Organic Electronics 15 (2014) 1476–1480

Contents lists available at ScienceDirect

Organic Electronics

journal homepage: www.elsevier.com/locate/orgel

Design rules for semi-transparent organic tandem solar cells for window integration

Jan Mescher [a,*], Siegfried W. Kettlitz [a], Nico Christ [a], Michael F.G. Klein [a], Andreas Puetz [a], Adrian Mertens [a], Alexander Colsmann [a], Uli Lemmer [a,b]

[a] Light Technology Institute (LTI), Karlsruhe Institute of Technology (KIT), Engesserstraße 13, D-76131 Karlsruhe, Germany
[b] Institute of Microstructure Technology (IMT), Karlsruhe Institute of Technology (KIT), Hermann-von-Helmholtz-Platz 1, D-76344 Eggenstein-Leopoldshafen, Germany

ARTICLE INFO

Article history:
Received 19 February 2014
Received in revised form 3 April 2014
Accepted 8 April 2014
Available online 24 April 2014

Keywords:
Color rendering index
Numerical simulation
Organic solar cell
Semi-transparency

ABSTRACT

For window integration of semi-transparent solar cells in living and working areas, color neutral transparency perception and good color rendering are of pivotal importance. In order to tune the optical device properties, we simulate a parallel tandem configuration with two different absorber materials. Within a regime of convenient transparency perception, the transparency can be adjusted between 20% and 40% by choosing the right absorber layer thickness combination. From the optical field in the tandem devices we calculate the charge carrier generation profile and subsequently correlate the optical properties with the electrical device properties as derived from drift-diffusion modelling – altogether allowing for a comprehensive assessment of the transparency, the transparency perception and the device performance and their interdependencies.

1. Introduction

The integration of semi-transparent organic solar cells (OSCs) into facades, overhead glazing or car windows is widely considered as key application for organic photovoltaics. So far, most scientific reports on semi-transparent solar cells focus on the fabrication and the optoelectronic properties of transparent top electrodes from conductive polymers such as poly(3,4-ethylenedioxy-thiophene):polystyrenesulfonate (PEDOT:PSS) [1–3], sputtered metal oxides such as aluminum doped zinc oxide (ZnO:Al) [4] or thermally evaporated ultra-thin metal layers such as silver (Ag) [5]. Other important aspects of semi-transparent solar cells that are of utmost importance for real-life applications outside the lab, are often not appreciated – among them their transparency color perception, i.e. a color neutral appearance, a convenient color temperature and good color rendering, or the trade-off between transparency and power conversion efficiency (PCE) [4,6]. Recently, we have demonstrated that the color rendering properties of semi-transparent solar cells can be tuned and improved by incorporating complementary absorbing dyes into the device and in particular into the polymeric electrode without affecting the device PCE [7]. Although the incorporation of dyes enables outstanding transparency color rendering properties, this approach cannot make use of the full device performance potential due to a loss of light to the dyes. Accordingly, better device performance can be achieved by employing a second complimentary absorber into the solar cell instead of a passive dye. This concept can be realized in semi-transparent tandem devices that combine two electrically active absorber materials with different absorption spectra, allowing simultaneous adjustment of the transparency color perception and enhancement in the PCE.

* Corresponding author. Tel.: +49 721 608 48587; fax: +49 721 608 42590.
E-mail addresses: Jan.Mescher@kit.edu (J. Mescher), Alexander.Colsmann@kit.edu (A. Colsmann).

http://dx.doi.org/10.1016/j.orgel.2014.04.011
1566-1199/

In this work we carry out a theoretic study of the design criteria for semi-transparent tandem solar cells with respect to the requirements for window integration. We examine the interplay of power conversion efficiency and transparency within a regime of convenient transparency color perception. Therefore, we simulate transmission spectra and current density–voltage (J–V) characteristics of tandem solar cells. Deliberately, we have chosen a parallel tandem architecture in three terminal configuration that decouples the optical and electrical properties. A tunable transparency allows for addressing different applications, e.g. integration into building facades or automotive windows.

2. Methods

For the simulation of the semi-transparent tandem solar cells and their transparency color perception we use an in-house developed software tool that employs transfer-matrix algorithms for an optical device description and drift-diffusion modelling [8] extended by a multi-trapping model for an electrical device property assessment [9,10]. The software tool was used to describe the opto-electronic properties of organic bulk heterojunction solar cells in the past [11]. The key to the quantitative analysis of the color properties of semi-transparent solar cells is their transmission spectrum. From the simulated transmission spectrum we calculate the chromaticity within the CIE 1931 and CIE 1960 UCS color space. According to the CIE 13.2 standard, we then determine the color rendering index (CRI) from the transmission spectrum [12]. The CRI describes the quality of color rendering for eight test color samples along the hue circle. Perfect color rendering is represented by a CRI of 100. For example, full spectrum fluorescent lamps can achieve a CRI $\approx$ 90. The human eye can distinguish CRI differences exceeding about 5. Further, we assess the corresponding color temperature (CCT) that is defined as the temperature of the black body radiator which chromaticity is closest to the chromaticity of the transmission spectrum [13]. Any CCT between 3300 K and 5000 K resembles natural white light and hence ensures comfortable illumination in general lighting [14]. According to the CIE standard, both CRI and CCT are valid if the displacement of the chromaticity of the investigated spectrum to the Planckian locus in the CIE 1960 UCS color space does not exceed $\Delta = 5.4 \times 10^{-3}$.

In addition to the transmission spectrum we use the overall device transparency as perceived by the human eye to describe the translucent properties of the device. This overall transparency is defined as the ratio of the incident and the transmitted luminous flux.

In serial tandem cells, the currents of the sub cells have to be matched to design properly working devices. Consequently, the thicknesses of the two absorption layers cannot be changed independently [5,15]. In parallel device configuration, the absorber layer thicknesses and hence the absorption can be adjusted over a wide range without respecting current matching, giving additional degrees of freedom for color tuning [16]. Therefore, our simulations deliberately focus on parallel connected tandem solar cells in three terminal configuration [17].

3. Results and discussion

In the following, we simulate 3-terminal (parallel) tandem solar cells comprising state-of-the-art conjugated polymer absorber materials, inspired by previous experimental work [18–21]. These tandem solar cells incorporate poly(3-hexylthiophene-2,5-diyl) and [6,6]-phenyl C_{61}-butyric acid methyl ester (P3HT:PC_{61}BM) as front (bottom) absorber layers and poly{[4,40-bis(2-ethylhexyl)dithieno(3,2-b;20,30-d)silole]-2,6-diyl-alt-(2,1,3-benzothidiazole)-4,7-diyl} and [6,6]-phenyl C_{71}-butyric acid methyl ester (PSBTBT:PC_{71}BM) as back (top) absorber layers. Both solar cells deliver approximately the same open circuit voltage V_{OC} for optimum parallel tandem performance. Fig. 1a shows the device architecture comprising a glass substrate, a 125 nm indium tin oxide (ITO) bottom anode, 40 nm molybdenum oxide (MoO_3), a P3HT:PC_{61}BM absorber layer with variable thickness, 10 nm zinc oxide (ZnO), a semi-transparent 12 nm common silver (Ag) cathode, 10 nm ZnO, a PSBTBT:PC_{71}BM absorber layer, again with variable thickness, 40 nm MoO_3 and finally a 60 nm ITO top anode. For optical simulations, the complex refractive indices of the active materials P3HT:PC_{61}BM and PSBTBT:PC_{71}BM in Fig. 1b were taken from literature [22] or were determined by spectroscopic ellipsometry (data will be published elsewhere). The refractive indices of MoO_3 and Ag were taken from literature [23,24]. The refractive indices of ITO and ZnO were determined by spectroscopic ellipsometry and are included in the supplementary information.

In order to study the interdependencies of the transparency, the PCE and the transparency color perception of the tandem solar cell, we vary the thicknesses of both absorber layers independently between 10 nm and 110 nm while keeping all other layer thicknesses of the device constant. All devices are virtually illuminated with an ASTM AM1.5 global standard spectrum. As we consider the transparency perception of pivotal importance for window integration, we first investigate the optical properties. The color changes from light yellow for thin P3HT:PC_{61}BM layers towards light purple for thin PSBTBT:PC_{71}BM layers. For further evaluation of the transmitted light, we assess Δ,

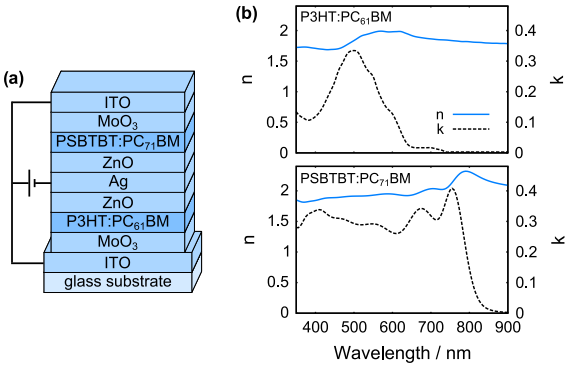

Fig. 1. (a) Device architecture of a parallel tandem solar cell comprising a ZnO/Ag/ZnO common middle cathode and ITO top and bottom anodes. (b) Refractive indices of P3HT:PC_{61}BM and PSBTBT:PC_{71}BM. Data taken from [22].

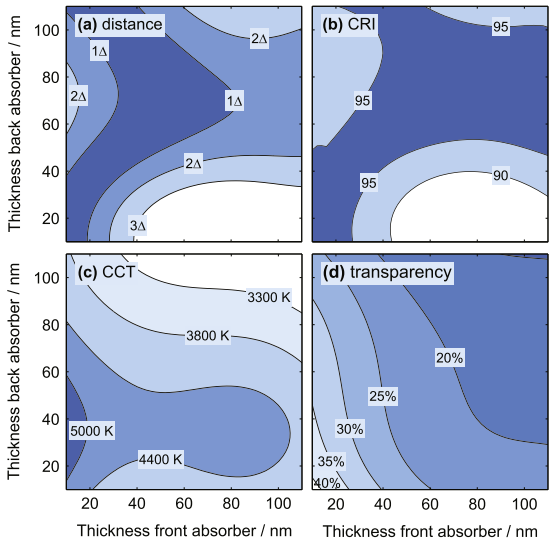

Fig. 2. Optical parameters of the tandem solar cells as a function of the layer thicknesses of the P3HT:$PC_{61}BM$ (front) and PSBTBT:$PC_{71}BM$ (back) layers: (a) chromaticity displacement to the Planckian locus, (b) CRIs, (c) CCTs and (d) transparency as calculated from the transmission spectrum.

CRI, CCT and the device transparency. Fig. 2a depicts the displacement of the transmission spectrum chromaticity from the Planckian locus Δ versus the thicknesses of the two absorber layers. The corresponding CRI and the CCT are shown in Fig. 2b and c, respectively. Fig. 2d shows the overall device transparency. All the optical data are valid for both front and back illumination due to the reversibility of the optical path. We chose the following target regimes for a convenient and color neutral light perception for all further considerations: $\Delta < 5.4 \times 10^{-3}$, CRI > 90 and 3300 K < CCT < 5000 K. $\Delta < 5.4 \times 10^{-3}$ is the mandatory condition for the determination of the CRI according to the CIE standard. A CRI beyond 90 characterizes light sources with color rendering properties surpassing most common light sources. A color temperature between 3300 K and 5000 K ensures convenient illumination.

Within this regime of convenient color perception, we find overall transparencies between 20% and 40% as illustrated in Fig. 2d. This tuning of the transparency while simultaneously preserving the excellent color properties allows addressing various technical applications that require different transparencies. To illustrate this wide range of achievable transparency levels, we exemplarily consider eight different active layer configurations (front/back absorber layer thicknesses) in this regime with transparencies between 40.1% and 19.3%: A: 12 nm/12 nm, B: 18 nm/22 nm, C: 24 nm/34 nm, D: 30 nm/46 nm, E: 38 nm/58 nm, F: 44 nm/70 nm, G: 50 nm/82 nm and H: 56 nm/94 nm. The corresponding CIE 1960 UCS chromaticities are depicted in Fig. 3 together with the Planckian locus (dashed line) and the chromaticities of black bodies with temperatures $T_1 = 3300$ K and $T_2 = 5000$ K, that mark the CCT range of the investigated configurations. The chromaticities of the samples A–H are located along the Planckian locus with their CCT decreasing from A to H. All configurations are within the CCT range for natural white.

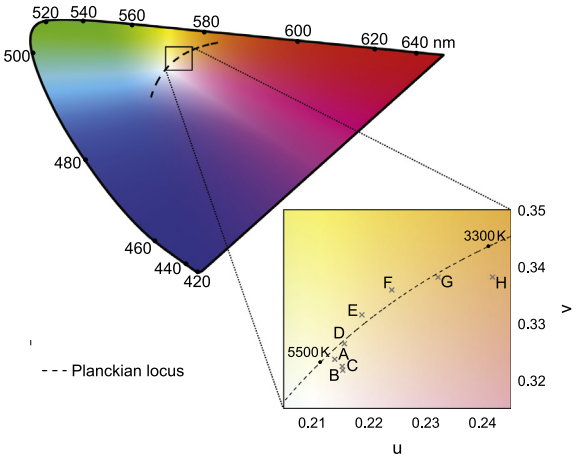

Fig. 3. Chromaticities of the tandem solar cells A–H in the CIE 1960 UCS color space. In the lower right part of the graph, the most relevant section has been enlarged.

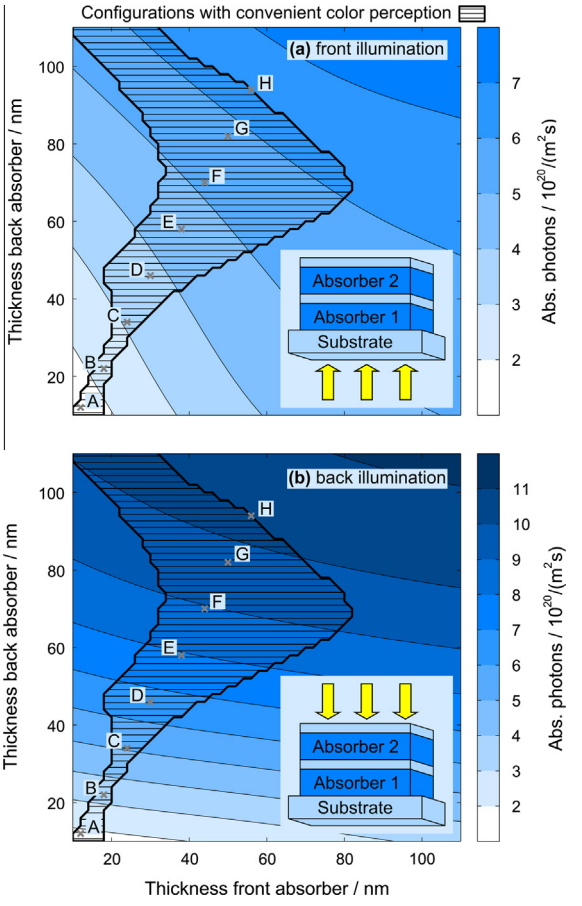

Fig. 4. Total number of absorbed photons in the two absorber layers as a function of the respective layer thicknesses under (a) front and (b) back illumination. The device configurations A–H are located within the regime of convenient transparency color perception (hatched, $\Delta < 5.4 \times 10^{-3}$, CRI > 90 and 3300 K < CCT < 5000 K). (For interpretation of the references to colour in this figure legend, the reader is referred to the web version of this article.)

While the transparency color perception of the semi-transparent devices does not depend on the direction of incidence due to the reversibility of the light path, it is important to understand that the electrical device properties can show a strong dependence. In general, under back illumination, the optical field distribution within the device and hence the absorption within the active layers, is different as compared to front illumination. Therefore, we correlate the optical and the electrical properties of our tandem solar cells by calculating the number of absorbed photons in both active layers under both directions of incidence. The sum of the number of absorbed photons in the two active layers as a function of the two absorber layer thicknesses is plotted in Fig. 4a and b for front and back illumination, respectively. In both figures, the regime of convenient color perception as defined before, has been hatched. We find that the number of absorbed photons in most our configurations is higher for back illumination. It is important to note that this observation cannot be generalized to other device architectures as the optical field distribution and hence the absorption profile in tandem solar cells depends strongly on the optical properties of the light harvesting and functional layers. Here, we particularly used a metal oxide/metal/metal oxide (ZnO/Ag/ZnO) intermediate electrode with reflection and transmission properties that strongly depend on the refractive indices and layer thicknesses. However, as a general outcome, power conversion in semi-transparent parallel tandem devices can change significantly upon flipping around the device while the transmission remains unaffected.

In order to obtain the PCEs of the devices A–H, we translate the numbers of absorbed photons under front and back illumination to charge carrier generation profiles and subsequently simulate the *J–V* characteristics of the two tandem subcells by drift-diffusion modelling. Then the *J–V* curve of the tandem device is calculated by adding the current densities of the two subcells for each voltage [16]. The *J–V* curves of the configuration F tandem cell under front and back illumination are exemplified in Fig. 5a. Fig. 5b shows the transparency (solid line) and the PCE of the tandem cells A–H under front (dashed line) and back illumination (dashed-dotted line). The PCE increases with decreasing transparency, from 0.5% to 3.1% under front illumination and from 0.6% to 4.6% under back illumination.

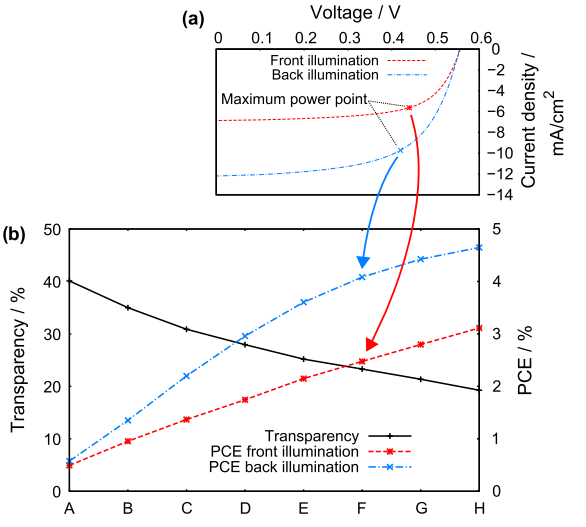

Fig. 5. (a) Simulated *J–V* characteristics of the configuration F tandem solar cell under front and back illumination. (b) Transparency and PCE under front and back illumination of the devices A–H.

The transmission target e.g. for car windows is typically around 25%. With the given pair of absorber polymers and the investigated device architecture, we find configuration F to best match all requirements of this particular application, i.e. the overall device transparency and a good transparency color perception while maintaining best efficiencies under back illumination of the device.

4. Conclusion

We present design considerations for semi-transparent organic tandem cells to target a certain transparency while preserving a good transparency color perception, i.e. a good color rendering and convenient color temperature. Parallel three-terminal architectures allow for more degrees of freedom than series connection. We exemplified our approach using P3HT:$PC_{61}BM$ and PSBTBT:$PC_{71}BM$ absorber layers. The presented methods can be applied to other combinations of absorber materials with complementary spectra and will yield similar results. This enables the design of semi-transparent devices with tailored optical properties in order to fulfill the strong requirements for window applications.

Acknowledgments

We acknowledge funding by the Federal Ministry of Education and Research (BMBF) under contract 03EK3501H (project POPUP). J.M. and M.F.G.K. thank the Karlsruhe School of Optics and Photonics (KSOP) for support.

Appendix A. Supplementary data

Supplementary data associated with this article can be found, in the online version, at http://dx.doi.org/10.1016/j.orgel.2014.04.011.

References

[1] T. Ameri, G. Dennler, C. Waldauf, H. Azimi, A. Seemann, K. Forberich, J. Hauch, M. Scharber, K. Hingerl, C.J. Brabec, Fabrication, optical modeling, and color characterization of semitransparent bulk-heterojunction organic solar cells in an inverted structure, Adv. Funct. Mater. 20 (10) (2010) 1592–1598.

[2] F. Nickel, A. Puetz, M. Reinhard, H. Do, C. Kayser, A. Colsmann, U. Lemmer, Cathodes comprising highly conductive poly(3,4-ethylenedioxythiophene):poly(styrenesulfonate) for semi-transparent polymer solar cells, Org. Electron. 11 (4) (2010) 535–538.

[3] Z. Tang, Z. George, Z. Ma, J. Bergqvist, K. Tvingstedt, K. Vandewal, E. Wang, L.M. Andersson, M.R. Andersson, F. Zhang, O. Inganaes, Semi-transparent tandem organic solar cells with 90% internal quantum efficiency, Adv. Energy Mater. 2 (12) (2012) 1467–1476.

[4] A. Bauer, T. Wahl, J. Hanisch, E. Ahlswede, ZnO:Al cathode for highly efficient, semitransparent 4% organic solar cells utilizing TiO_x and aluminum interlayers, Appl. Phys. Lett. 100 (7) (2012). 073307–3.

[5] J. Meiss, T. Menke, K. Leo, C. Uhrich, W.-M. Gnehr, S. Sonntag, M. Pfeiffer, M. Riede, Highly efficient semitransparent tandem organic

solar cells with complementary absorber materials, Appl. Phys. Lett. 99 (4) (2011) 043301–043303.
[6] A. Colsmann, A. Puetz, A. Bauer, J. Hanisch, E. Ahlswede, U. Lemmer, Efficient semi-transparent organic solar cells with good transparency color perception and rendering properties, Adv. Energy Mater. 1 (4) (2011) 599–603.
[7] J. Czolk, A. Puetz, D. Kutsarov, M. Reinhard, U. Lemmer, A. Colsmann, Inverted semi-transparent polymer solar cells with transparency color rendering indices approaching 100, Adv. Energy Mater. 3 (2012) 386–390.
[8] C. Pflumm, C. Gärtner, U. Lemmer, A numerical scheme to model current and voltage excitation of organic light-emitting diodes, IEEE J. Quantum. Electron. 44 (8) (2008) 790–798.
[9] N.S. Christ, S.W. Kettlitz, S. Valouch, S. Züfle, C. Gärtner, M. Punke, U. Lemmer, Nanosecond response of organic solar cells and photodetectors, J. Appl. Phys. 105 (10) (2009) 104513–104522.
[10] N. Christ, S.W. Kettlitz, S. Zü fle, S. Valouch, U. Lemmer, Nanosecond response of organic solar cells and photodiodes: role of trap states, Phys. Rev. B 83 (19) (2011) 195211.
[11] N. Christ, S.W. Kettlitz, S. Valouch, J. Mescher, M. Nintz, U. Lemmer, Intensity dependent but temperature independent charge carrier generation in organic photodiodes and solar cells, Org. Electron. 14 (3) (2013) 973–978.
[12] Commission Internationale de l'Éclairage International, Cie 13.3.
[13] N. Lynn, L. Mohanty, S. Wittkopf, Color rendering properties of semi-transparent thin-film PV modules, Build. Environ. 54 (2012) 148–158.
[14] E. Theiß, Gebäudetechnik, vol. 1: Beleuchtungstechnik: neue Technologien der Innen- und Außenbeleuchtung, Oldenbourg-Industrieverl., München, 2000.
[15] N.-K. Persson, O. Inganäs, Organic tandem solar cells – modelling and predictions, Sol. Energy Mater. Sol. Cells 90 (20) (2006) 3491–3507.
[16] P. Peumans, A. Yakimov, S.R. Forrest, Small molecular weight organic thin-film photodetectors and solar cells, J. Appl. Phys. 93 (7) (2003) 3693–3723.
[17] S. Sista, Z. Hong, M.-H. Park, Z. Xu, Y. Yang, High-efficiency polymer tandem solar cells with three-terminal structure, Adv. Mater. 22 (8) (2010) E77–E80.
[18] A. Puetz, F. Steiner, J. Mescher, M. Reinhard, N. Christ, D. Kutsarov, H. Kalt, U. Lemmer, A. Colsmann, Solution processable, precursor based zinc oxide buffer layers for 4.5% efficient organic tandem solar cells, Org. Electron. 13 (11) (2012) 2696–2701.
[19] K.-S. Chen, J.-F. Salinas, H.-L. Yip, L. Huo, J. Hou, A.K.-Y. Jen, Semi-transparent polymer solar cells with 6% PCE, 25% average visible transmittance and a color rendering index close to 100 for power generating window applications, Energy Environ. Sci. 5 (11) (2012) 9551–9557.
[20] H. Schmidt, H. Flugge, T. Winkler, T. Bulow, T. Riedl, W. Kowalsky, Efficient semitransparent inverted organic solar cells with indium tin oxide top electrode, Appl. Phys. Lett. 94 (24) (2009) 243302–243303.
[21] Y. Ka, E. Lee, S.Y. Park, J. Seo, D.-G. Kwon, H.H. Lee, Y. Park, Y.S. Kim, C. Kim, Effects of annealing temperature of aqueous solution-processed ZnO electron-selective layers on inverted polymer solar cells, Org. Electron. 14 (1) (2013) 100–104.
[22] G. Dennler, K. Forberich, T. Ameri, C. Waldauf, P. Denk, C.J. Brabec, Design of efficient organic tandem cells: on the interplay between molecular absorption and layer sequence, J. Appl. Phys. 102 (2007) 123109.
[23] A. Abdellaoui, G. Lévêque, A. Donnadieu, A. Bath, B. Bouchikhi, Iteratively derived optical constants of MoO3 polycrystalline thin films prepared by CVD, Thin Solid Films 304 (1997) 39–44.
[24] E.D. Palik, Handbook of Optical Constants of Solids, Academic Press, 1998.